involving ester group k depends therefore on the torsional angles of skeletal bonds within both of the adjoining diads and on χ_{k-1} and χ_{k+1} as well as on χ_k. A complete accounting of the influences of these parameters incident to a given ester group would be beyond reach of any manageable treatment.
(24) Vacatello, M.; Flory, P. J. *Polym. Commun.* **1984**, *25*, 258.
(25) Kusanagi, H.; Tadokoro, H.; Chatani, Y. *Macromolecules* **1976**, *2*, 531.
(26) Lovell, R.; Windle, A. H. *Polymer* **1981**, *22*, 175.
(27) Flory, P. J. *Macromolecules* **1974**, *7*, 381.
(28) Sakurada, I.; Nakajima, A.; Yoshizaki, O.; Nakamae, K. *Kolloid Z.* **1962**, *186*, 41.
(29) Shulz, G. V.; Wunderlich, W.; Kirste, R. *Makromol. Chem.* **1964**, *75*, 22.
(30) Moore. W. R.; Fort, R. F. *J. Polym. Sci., Part A* **1963**, *1*, 929.
(31) Jenkins, R.; Porter, R. S. *Polymer* **1982**, *23*, 105.
(32) Krause, S.; Cohn-Ginsberg, E. *J. Phys. Chem.* **1963**, *67*, 1479.
(33) Vadusevan, P.; Santappa, M. *J. Polym. Sci., Part A-2* **1971**, *9*, 483.
(34) Chinai, S. N.; Valles, R. J. *J. Polym. Sci.* **1959**, *39*, 363.
(35) Fox, T. G. *Polymer* **1962**, *3*, 111.
(36) Yoon, D. Y.; Flory, P. J. *Macromolecules* **1976**, *9*, 299.
(37) Kirste, R. G. *Makromol. Chem.* **1967**, *101*, 91.
(38) Kirste, R. G.; Kruse, W. A.; Ibel, K. *Polymer* **1975**, *16*, 120.

Conformational Analysis of Poly(methyl methacrylate)

P. R. Sundararajan

Xerox Research Centre of Canada, 2660 Speakman Drive, Mississauga, Ontario L5K 2L1, Canada. *Received April 2, 1985*

ABSTRACT: Conformational energies associated with the various states of the meso and racemic diads of poly(methyl methacrylate) have been estimated. The skeletal bond angle at the methylene carbon atom and the side-group torsion angles were varied in order to minimize the energy at each of the skeletal conformations defined by φ_i and φ_{i+1}. In contrast to the previous calculations with fixed side-group torsion angles, the present results show that the $\bar{g}$ conformation is accessible to the chain. Agreement between the experimental and theoretical values of the characteristic ratio $\langle r^2\rangle_0/nl^2$, for the isotactic chain, is achieved if the tt state is treated with $(\varphi_i, \varphi_{i+1}) = (10°, -15°)$, leading to helical segments with a large pitch. The energy differences between the various states estimated from the calculations are compared with the values derived from FTIR experiments.

Introduction

Calculations on the conformational energies of the various states accessible to the poly(methyl methacrylate) (PMMA) chain have been reported by Sundararajan and Flory.[1,2] The $\bar{g}$ state was ruled out, leading to a two-state scheme (involving t and g) for the formulation of the statistical weight matrices and the calculation of the characteristic ratio and its temperature coefficient. The energy parameters derived from this work have been used by various authors to calculate properties of the PMMA chain such as the small-angle X-ray and neutron scattering curves,[3] wide-angle X-ray scattering[4] from amorphous PMMA, the average dipole moment,[5] persistance vectors,[6] etc. The characteristic ratios calculated for the stereoirregular chains have been compared with recent experimental results.[7,8]

While calculations such as the characteristic ratios and scattering curves depend on the energy parameters derived from conformational analysis, direct derivation of differences in energies between various states of the chain has been reported by O'Reilly and co-workers,[9,10] using FTIR methods. Measurements were carried out on both hydrogenated and deuterated isotactic, syndiotactic, and atactic PMMA. The energies were assigned on the basis of the two-state (tt and tg/gt) model. It was also possible to separate the energies associated with the backbone and side chains. The agreement with previous calculations was good in the case of syndiotactic PMMA but not for the isotactic case.[9] Further, the experiments on deuterated PMMA prompted the suggestion[10] that additional gauche states might be accessible to PMMA.

Considering the active interest in the estimation of energy differences between various states of PMMA, arising from short-range interactions, the calculations of conformational energies were reexamined. Allowance was made for the variation of the skeletal bond angle $C^\alpha CC^\alpha$ and the side-group torsion angles. The present calculations indicate the accessibility of additional states when variations in such geometrical parameters are taken into account.

Description of Calculations

The various geometrical parameters are defined in the schematic shown in Figure 1. The bond lengths and bond angles were chosen as before[1] except that the angle θ'' was varied from 118 to 126°, in steps of 2°, at each of the $(\varphi_i, \varphi_{i+1})$ conformations. The enlargement of the angle θ'' from tetrahedral value, in order to accommodate the large size of the side groups, has been discussed before.[1] The CH_2 and CH_3 groups were treated as hard spheres except for the methylene group $(CH_2)_i$. As the value of θ'' was varied from 118° to 126°, for each θ'', the two hydrogen atoms of the methylene group were located such that the angles $C^\alpha_{i-1}C_iH_i$, $C^\alpha_{i-1}C_iH_i$*, $C^\alpha_{i+1}C_iH_i$, $C^\alpha_{i+1}C_iH_i$* and $H_iC_iH_i$* are equal and denoted by θ. Modification of eq 2 of Suter and Flory[11] to this end leads to

$$\cos\theta = \frac{1 \pm (1 + 4x)^{1/2}}{2x} \tag{1}$$

where

$$x = 4/(1 + \cos\theta'') \tag{2}$$

The side-group torsion angles χ_{i-1} and χ_{i+1} were taken to be 0° when the carbonyl bond eclipses the C^α–CH_3 bond. The angles χ_{i-1} and χ_{i+1} were varied, in steps of 10^0 in the ranges of −40° to +40° and 140° to 220°, corresponding to the "up" and "down" configurations of the carbonyl bond. Values of χ outside these ranges were considered unlikely. (This restriction gave rise to a problem in certain conformations such as $\bar{g}\bar{g}$. A well-defined minimum for (χ_{i-1}, χ_{i+1}) was not reached within the above range in these cases. Further analysis showed that a minimum is reached about 10° beyond the above range, although the energy decreased by only a few cal mol^{-1}. In such cases, the least energy corresponding to the extremities of the above range

0024-9297/86/2219-0415$01.50/0

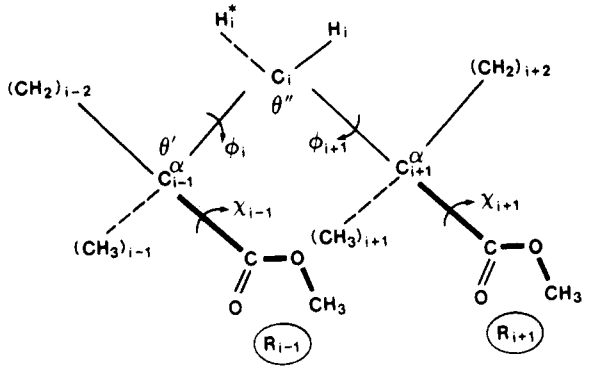

Figure 1. Schematic of a diad of PMMA, with the various geometrical parameters used for the calculations.

Table I
Average Parameters Derived from Energy Calculations

state	z	$\langle E \rangle$	$\langle \theta'' \rangle$	$\langle \varphi_i, \varphi_{i+1} \rangle$
		meso		
tt	21.98	0.44	123.6	−2.8, −2.8
tg	4.15	1.32	124.8	1.8, 112.8
t$\bar{g}$	4.45	1.21	123.9	−4.1, −115.8
gg	0.31	3.00	125.7	119.3, 119.3
g$\bar{g}$	0.89	2.08	124.7	113, −109.4
$\bar{g}\bar{g}$	0.35	2.85	125.0	−118.3, −118.3
		racemic		
tt	29.62	0.11	123.4	1.7, 1.7
tg	3.35	1.52	124.8	−4.2, 119.2
t$\bar{g}$	7.91	0.85	124.0	3.5–109.9
gg	0.43	2.68	125.5	111.9, 111.9
g$\bar{g}$	0.54	2.62	124.9	124.0, −111.1
$\bar{g}\bar{g}$	0.67	2.11	124.2	−111.9, −111.9

was taken, since significant reduction in energy has been achieved by a rotation of 40° from perfect eclipsed position.) Thus, both the skeletal bond angle θ'' and (χ_{i-1}, χ_{i+1}) were varied for each of the $(\varphi_i, \varphi_{i+1})$ conformations to minimize the energy. The torsion angles φ_i and φ_{i+1} were varied at intervals of 5° each.

The energy parameters were chosen as before.[1] The nonbonded and Coulombic interactions, torsional contributions, and energy due to bond angle deformation were included in calculating the energy.

Results of Energy Calculations

The energy contours for the various states of the meso and racemic diads are shown in Figures 2 and 3, respectively. The partition functions z for the various states, by taking the sums of the Boltzmann factors of the energy at intervals of 5° over the various domains,[1] the averages of the energy $\langle E \rangle$, the bond angle $\langle \theta'' \rangle$, and the torsion angles $\langle \varphi_i, \varphi_{i+1} \rangle$ are given in Table I.

Table I shows that the value of $\langle \theta'' \rangle$ varies from 123.4° to 125.7°. The $\bar{g}$ state is not of high energy and the energies of the tg and t$\bar{g}$ states are comparable for the meso diad. The energy of the t$\bar{g}$ state, in the case of the racemic diad, is lower than that of tg. The reduction in the energy of the t$\bar{g}$ state, compared with the previous work,[1] is a consequence of enlargement of the angle θ'' to 124° and allowing for variations in χ.

The minima in Figures 2 and 3 are shifted from perfect staggering, by about 10–15° in φ_i and φ_{i+1}. Shifts greater than ~15° are not favorable due to the increase in "diagonal interactions", as discussed before.[1,12] Diagonal interactions are those that occur between atoms or groups appended to C^α_{i-1} and those attached to C^α_{i+1} and situated on opposite sides of the plane of the skeletal bonds. For example, in the tt state of the meso diad, the interaction between $(CH_3)_{i-1}$ and $(COOCH_3)_{i+1}$ is a diagonal interaction. In the case of meso tt, gg, $\bar{g}\bar{g}$, and racemic tg, minima are situated symmetrically on either side of the perfectly staggered position. This is due to the equivalence of the interactions for the respective shifts. In the case of the

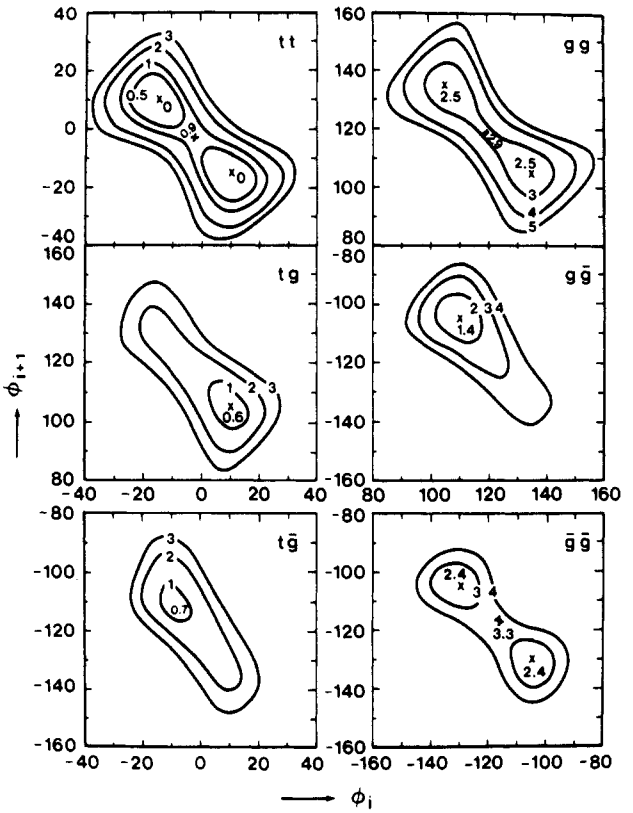

Figure 2. Energy contours (kcal mol^{-1}) for the various states of the meso diad of PMMA. Contours are shown relative to the minimum corresponding to the tt state taken as zero.

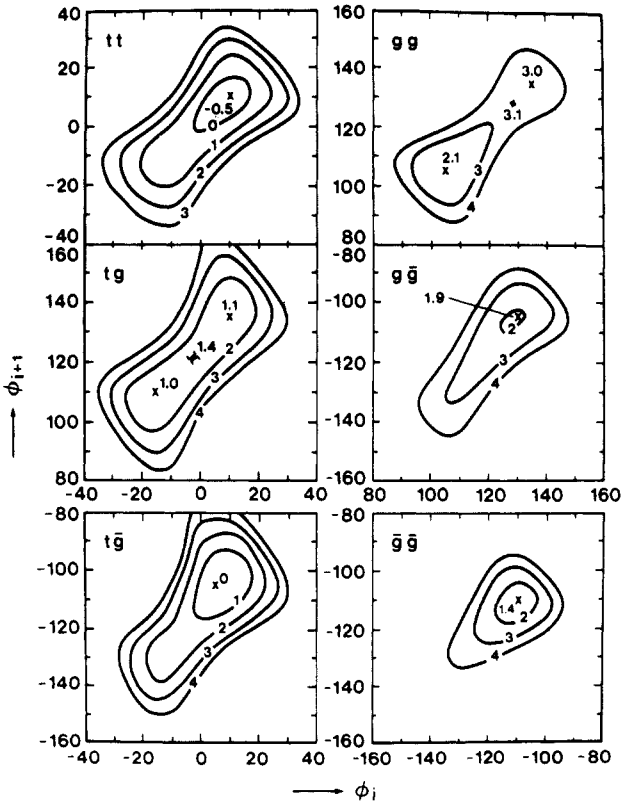

Figure 3. Energy contours (kcal mol^{-1}) for the various states of the racemic diad of PMMA. Contours are shown relative to the minimum corresponding to the meso, tt state taken as zero.

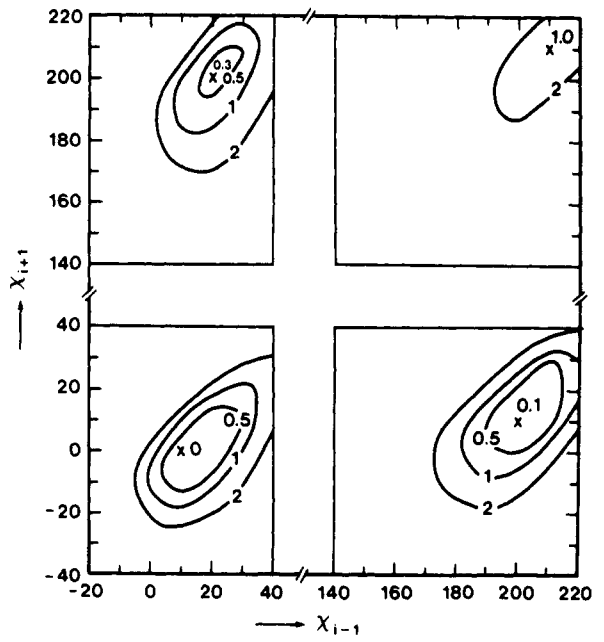

Figure 4. Energy contours (kcal mol^{-1}) in terms of χ_{i-1} and χ_{i+1} are shown, corresponding to the skeletal conformation of the meso diad with $(\varphi_i, \varphi_{i+1}) = (10°, -15°)$. For convenience, the range from −180 to −140° has been shown as from 180° to 220°.

meso diad, the shifts $\Delta\varphi_i$ and $\Delta\varphi_{i+1}$, in all the states, are of opposite sign. Shifts of the same sign give rise to higher energy. This is a significant difference between disubstituted chains such as PMMA and poly(α-methylstyrene)[12] and monosubstituted chains, e.g., polystyrene[13] and poly(*N*-vinylcarbazole)[14]. In the case of the latter class, shifts of the same sign are preferred.

The perpetuation of conformations with (+, −) or (−, +) shifts, in the region of the tt state, generates helices with a large pitch. For example, with $(\varphi_i, \varphi_{i+1}) = (10°, -15°)$ or (−15°, 10°) and $\theta'' = 124°$, a helix with 14 monomers per turn, with a pitch of 30.4 Å, will result. If the shifts $\Delta\varphi_i$ and $\Delta\varphi_{i+1}$ are of the same sign, cyclic structures would be generated. For all the conformations defined by $\varphi_i = \varphi_{i+1}$, the pitch would be zero, with the chain closing upon itself with varying number of residues. The number of residues sufficient for chain closure would depend on the difference between the angles θ' and θ'' and the values of φ_i and φ_{i+1}. In the case of the racemic diad (Figure 3), the shifts of the minima from perfect staggering are of the same sign in $\Delta\varphi_i$ and $\Delta\varphi_{i+1}$.

For illustration, the energy map in terms of (χ_{i-1}, χ_{i+1}) corresponding to the minimum in φ_i and φ_{i+1} for the meso tt state is shown in Figure 4. The minima occur at $(\chi_{i-1}, \chi_{i+1}) = (10°, 0°)$, (20°, −160°), (−150°, −150°) and (−160°, 10°), the first being the most favorable. It is seen that the range of accessible conformations of χ, within, say, 1 kcal mol^{-1}, is restricted to about 20° in the carbonyl "up" and "down" configurations. This range was found to be larger (about 40°) in the case of the meso tg state.

Statistical Weights

Following the previous discussion,[15] the statistical weight matrix **U′** for the bond pair $i-1$ and i is given by

$$\mathbf{U}' = \begin{bmatrix} 1 & 1 & 1 \\ 1 & 0 & \psi \\ 1 & \psi & 0 \end{bmatrix} \tag{3}$$

In this rendition, all the first-order statistical weights have been transferred to the matrix **U″** for the bond pair i, $i+1$. As discussed before,[15] the conformations g|$\bar{g}$ and $\bar{g}$|g of bonds $i-1$ and i give rise to interactions between groups separated by six bonds. These interactions depend on the states of the bonds $i-2$ and $i+1$ as well as those of $i-1$ and i and hence are fourth-order interactions. Inasmuch as the groups involved in the interactions are large and are not distinguished here, a statistical weight ψ is assigned to such interactions. Direct determination of ψ is not feasible with the energy calculations performed here on the conformations of bonds i and $i+1$. Since the interactions defined by ψ are expected to be significant, a value of 2.5 kcal mol^{-1} is assigned for E_ψ.

For the second-order interactions, we assign a statistical weight ω'' for the interaction R···R, ω' for R···CH_2 or CH_3, and ω for CH_2 or CH_3···CH_2 or CH_3. The statistical weight matrix for the bond pair i, $i+1$ of the meso and racemic diads, including the first- and second-order interactions is then given by[15]

$$\mathbf{U''}_m = \begin{bmatrix} \eta^2\omega\omega'' & \eta\omega\omega' & \eta\tau\omega'^2 \\ \eta\omega\omega' & \omega^2 & \tau\omega\omega' \\ \eta\tau\omega'^2 & \tau\omega\omega' & \tau^2\omega\omega'' \end{bmatrix} \tag{4}$$

and

$$\mathbf{U''}_r = \begin{bmatrix} \eta^2\omega'^2 & \eta\omega\omega' & \tau\eta\omega\omega'' \\ \eta\omega\omega' & \omega^2 & \tau\omega\omega' \\ \eta\tau\omega\omega'' & \tau\omega\omega' & \tau^2\omega'^2 \end{bmatrix} \tag{5}$$

The five statistical weights can be reduced to three by defining

$$\alpha = \omega'/\eta\omega''$$

$$\beta = \omega'^2/\omega\omega''$$

$$\rho = \tau/\eta \tag{6}$$

Then, eq 4 and 5 reduce to

$$\mathbf{U''}_m = \begin{bmatrix} 1 & \alpha & \beta\rho \\ \alpha & \alpha^2/\beta & \alpha\rho \\ \beta\rho & \alpha\rho & \rho^2 \end{bmatrix} \tag{7}$$

$$\mathbf{U''}_r = \begin{bmatrix} \beta & \alpha & \rho \\ \alpha & \alpha^2/\beta & \alpha\rho \\ \rho & \alpha\rho & \beta\rho^2 \end{bmatrix} \tag{8}$$

The energies corresponding to the three statistical weights can be determined by combining the elements of each state of the statistical weight matrices $\mathbf{U''}_m$ and $\mathbf{U''}_r$ and the average energies $\langle E \rangle$ given in Table I for the respective states. A suitable method to this end has been described by Suter and Flory.[11] If any one of the statistical weight parameters is given by ξ and $\langle E \rangle_s$ is the energy of the state s, the energy E_ξ corresponding to the parameter ξ is given by the solution of the overdetermined set of 11 linear equations

$$\sum E_\xi - \langle E \rangle_s = 0 \tag{9}$$

The 11 equations are comprised of the nonequivalent states of the meso and racemic diads, with the exclusion of the meso tt state, which has a weight of one.

The differences in the shape and size of the energy domains between the various states are taken into account[11] by introducing a preexponential factor ξ_0, such that

$$\xi = \xi_0 \exp(-E_\xi/RT) \tag{10}$$

The values of ξ_0 corresponding to the three statistical weight parameters can be deduced from the set of 11 linear equations

$$\sum \ln \xi_0 - \ln z_s - (\sum E_\xi/RT) = 0 \tag{11}$$

Table II
Energies (kcal mol^{-1}) Corresponding to the Backbone and Side-Chain Interactions in the Meso Diad of PMMA

state	$\langle E \rangle_{tot}$	E^{min}_{tot}	E^{min}_{bb}	E^{min}_{SC}
tt	0.44	20.19	21.69	−1.50
tg	1.32	20.83	20.41	0.42
tḡ	1.21	20.92	19.85	1.06
gg	3.00	22.70	21.25	1.45
gḡ	2.08	21.59	19.94	1.65
ḡḡ	2.85	22.60	21.65	0.95

Table III
Relative Energies (kcal mol^{-1}) of the Four Generic Conformations of the Side Groups in the Various Skeletal States of the Meso Diad of PMMA

state	uu	ud	dd	du
tt	0	0.3	1.0	0.1
tg	0.1	0	0.9	1.0
tḡ	0.2	0	0.8	1.3
gg	0	0	0.5	0.4
gḡ	0.7	0.2	0	0.5
ḡḡ	6.2	1.0	0	2.2

The above procedure leads to the following values for the statistical weights:

$$\alpha = 0.85 \exp(-991/RT)$$

$$\beta = 0.77 \exp(358/RT)$$

$$\rho = 0.87 \exp(-1016/RT) \quad (12)$$

Comparison with FTIR Experimental Results

O'Reilly and Mosher derived the difference in the conformational energy between tt and tg states of i-, s-, and a-PMMA, using the FTIR technique.[9] On the basis of previous calculations,[1] they assumed a two-state scheme (tt and tg or gt) for the conformational states. The large energy difference, ΔH deduced from the 1276/1264-cm^{-1} band pair was assigned to the backbone conformational change. The four sets of bands from 1276 to 1136 cm^{-1}, recorded below T_g, were used to estimate the energy difference in side-group conformations. O'Reilly and Mosher proposed two models for the assignment of the energies since associating the latter with the backbone, side-chain, and combined total contributions, could not be done unambiguously.

Table II shows the values of $\langle E \rangle$ at 300 K, and the energy E at the minimum in the $(\varphi_i, \varphi_{i+1})$ map corresponding to each state of the meso diad. The values of E have been further divided into the energy E_{bb} due to backbone (including the α-methyl) interactions and E_{SC} due to the side chain, corresponding to the energy of interaction of the R_{i-1} and R_{i+1} groups between themselves and with the rest of the diad. The value of E_{SC} refers to the energy at the minimum in the (χ_{i-1}, χ_{i+1}) map calculated for the $(\varphi_i, \varphi_{i+1})$ at the minimum for each of the states of the bonds i and $i + 1$. For example, E_{SC} = −1.5 kcal mol^{-1} given for the tt state in Table II corresponds to $(\chi_{i-1}, \chi_{i+1}) = (10°, 0°)$ (see Figure 4) with $(\varphi_i, \varphi_{i+1}) = (10°, -15°)$ (see Figure 2). From Table II, the values of $\Delta\langle E \rangle$ and ΔE between tt and tg states are 880 and 640 cal mol^{-1}, respectively. The energy difference between tt and tḡ is 760 cal. mol^{-1} on the basis of $\Delta\langle E \rangle$ and 730 cal mol^{-1} according to ΔE. All these values are in good agreement with the value of 720 cal mol^{-1} derived from FTIR measurements. If the values of E_{bb} are considered, the energy difference between tt and tg; tt and tḡ, and tg and tḡ are 1280, 1840, and 560 cal mol^{-1}, respectively. It is seen from Table II that on the basis of the backbone energies alone, the tt conformation is higher in energy than tg or tḡ. However,

Table IV
Energies (kcal mol^{-1}) Corresponding to the Backbone and Side-Chain Interactions in the Racemic Diad of PMMA

state	$\langle E \rangle_{tot}$	E^{min}_{tot}	E^{min}_{bb}	E^{min}_{SC}
tt	0.11	19.7	19.44	0.26
tg	1.52	21.21	19.96	1.25
tḡ	0.84	20.23	21.67	−1.44
gg	2.68	22.26	21.25	1.01
gḡ	2.62	22.14	19.94	2.20
ḡḡ	2.11	21.63	19.84	1.79

Table V
Relative Energies (kcal mol^{-1}) of the Four Generic Conformations of the Side Groups in the Various Skeletal States of the Racemic Diad of PMMA

state	uu	ud	dd	du
tt	0	0.9	1.9	0.9
tg	0.2	0	0.8	1.0
tḡ	0	0.3	0.5	1.0
gg	0	0	0.1	0
gḡ	0.6	0.1	0	0.5
ḡḡ	1.1	0.3	0	0.3

the side-group interaction in the tt state is more favorable than in the tg or tḡ state, leading to a lower total energy of the tt state. Thus, it is likely that the energy difference measured from FTIR for i-PMMA, above T_g, corresponds to the total energy.

Table III shows the relative energies of the various side-group conformations, corresponding to each state of the meso diad. The side-group conformations (of R_{i-1} and R_{i+1}) are generically denoted by u (carbonyl "up") and d (carbonyl "down") in this table. The energies are listed for each side-group conformation relative to the minimum (E_{SC} in Table II) in the χ_{i-1}, χ_{i+1} map in each state taken as zero. It is seen that except in the ḡḡ state, the energy difference between the four generic conformations is within 1 kcal mol.$^{-1}$ This is applicable to the case in which the backbone conformation does not change. If it does, and if the energy attributable to the side group in such conformational change can be estimated experimentally, it can be compared with the differences in the values of E_{SC} given in Table II. Results are not available from FTIR measurements, for the side-group energies, since the experiments were not carried out below T_g for i-PMMA.

Tables IV and V are similar to Tables II and III, respectively, but for the case of the racemic diad. The energy difference between tt and tg states is 1410 cal mol^{-1} on the basis of $\Delta\langle E \rangle$ and 1510 cal mol^{-1}, with ΔE. The values of $\Delta\langle E \rangle$ and ΔE between tt and tḡ states are 730 cal mol^{-1} and 530 cal mol^{-1}, respectively. If the tg and tḡ states are compared, $\Delta\langle E \rangle$ and ΔE are 680 and 980 cal mol^{-1}, respectively. On the basis of the backbone energy E_{bb}, the differences between tt and tg, tt and tḡ, and tg and tḡ are 520, 2230, and 1710 cal mol^{-1}, respectively. The energies derived from FTIR measurements are as follows: An energy of ΔE = 2000 cal mol^{-1}, is attributable to ΔE_{bb} as per Model I or to $\Delta E_{bb} + \Delta E_{SC}$ according to Model II, based on the two-state (tt and tg) scheme; an energy of 1164 cal mol^{-1} was assigned to $\Delta E_{bb} - \Delta E_{SC}$ in Model I and to ΔE_{bb} in Model II. The calculated energies of 2230, 1410, 1510, and 1710 cal mol^{-1} described above are close to the values of 2000 ± 222 and 1164 ± 80 cal mol^{-1} derived from FTIR. The conformational energy differences calculated from Table IV, viz., $\Delta\langle E \rangle$ = 730 cal mol^{-1} and ΔE = 530 cal mol^{-1} between tt and tḡ, ΔE_{bb} = 520 cal mol^{-1} between tt and tg, and $\Delta\langle E \rangle$ = 680 and ΔE = 980 cal mol^{-1} between tt and tḡ have to be accounted for from FTIR experiments.

Table V lists the relative energies of the four generic side-group conformations in each of the states of the

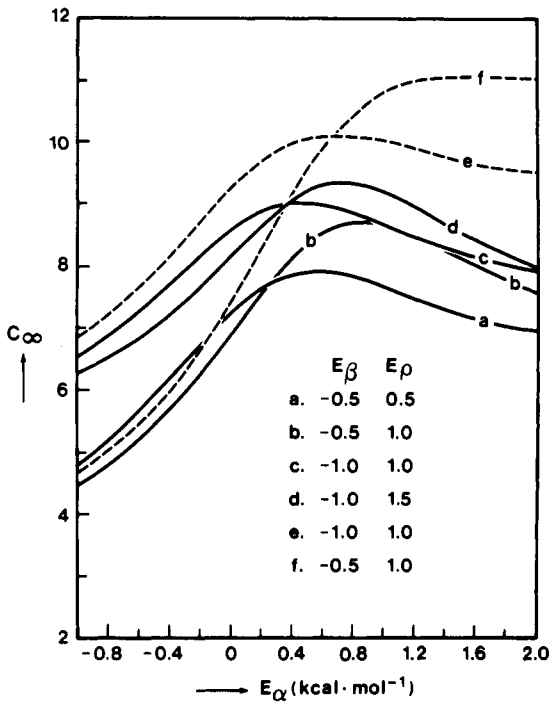

Figure 5. The characteristic ratio C_∞ for isotactic PMMA is shown as a function of E_α, for select values of E_β and E_ρ. The solid curves correspond to φ_i, φ_{i+1} = -5°, -5° for the meso, tt state and the dashed curves to φ_i, φ_{i+1} = 10°, -15°.

skeletal bonds of the racemic diad. It is seen that with the exception of the "down–down" configuration in the tt state, all the energy differences are within 1000 cal mol^{-1}. This agrees well with the energy of 835 ± 100 cal mol^{-1} assigned to ΔE_{SC} from FTIR measurements.

Characteristic Ratios

Characteristic ratios for stereoregular and stereoirregular chains were calculated according to methods described previously.[13,15,16] The values of $\langle \varphi_i, \varphi_{i+1} \rangle$ given in Table I were used for the various states, after rounding off to the nearest 5°. Since the values of $\langle \theta'' \rangle$ are close to 124° in the various conformations, the same value was used throughout. Although the value of E_ψ is not determined directly from the above calculations, in view of the intensity of the interactions that it represents, a value of 2500 cal mol^{-1} was assigned to this parameter.

Characteristic ratios calculated for the i-PMMA chain, as a function of E_α are shown in Figure 5. Such plots of C_∞ in terms of various values of E_α enable understanding of the effect of the population of the various conformers on C_∞. Curves are shown in Figure 5, corresponding to select values of E_β and E_ρ. It is seen that C_∞ increases with E_α up to $E_\alpha \approx 1$ kcal mol^{-1} and decreases thereafter. The tg (or gt) conformation depends on E_α. When E_α is large, the predominance of the tt conformation, with $\langle \varphi_i, \varphi_{i+1} \rangle$ = (-5°, -5°) promotes looping of the chain, since $\theta' \neq \theta''$. As E_α decreases, more tg states are available and C_∞ increases owing to the decreased incidence of looping, reaching a maximum at $E_\alpha \approx 1$ kcal mol^{-1}. The decrease in C_∞ with a further decrease in E_α is attributed to the disorder caused by interspersion of numerous bond pairs in the tg state. The t$\bar{g}$ conformation depends on both E_β and E_ρ. A comparison of curves b and c in Figure 5 shows that an increase in E_β reduces the value of C_∞. Apart from influencing the incidence of t$\bar{g}$, an increase in E_β also increases the occurrence of the gg state. Curves a and b, with E_β = -0.5 kcal mol^{-1}, show that decreasing the value of E_ρ decreases C_∞ for $E_\alpha > 0.2$ kcal mol^{-1}. One might expect that a decrease in E_ρ and the resultant increase in the incidence of the t$\bar{g}$ conformation would increase C_∞ due to the prevention of looping. The opposite behavior seen in the results can be interpreted as due to the contributions from such states as g$\bar{g}$ and $\bar{g}\bar{g}$. The extent of reduction in the value of C_∞ due to a change in E_ρ depends on the value of E_β. This is evident by comparing curves a and b with c and d in Figure 5.

The experimental values[7,8] of C_∞ for predominantly isotactic PMMA are in the range of 9.2–10.7. The recent work of Jenkins and Porter[8] shows that C_∞ varies from 9.3 to 10.2 as the isotacticity increases from 83 to 100%. The solid curves in Figure 5 show that the value of C_∞ does not exceed 9.3. Reasonable adjustment of the statistical weight parameters failed to increase C_∞ to match the experimental values. Compared with the previous work,[1] the reduction in the calculated values of C_∞ is due to the inclusion of the $\bar{g}$ state. Thus, the experimental values of $9.2 \leq C_\infty \leq 10.7$ are not accounted for by the solid curves in Figure 5. However, good agreement with the experimental results can be obtained by considering certain features of the conformations of the chain, as discussed below.

On the basis of the results shown in Table I, $\langle \varphi_i, \varphi_{i+1} \rangle$ = (-5°, -5°) was used above for the meso, tt state to calculate C_∞. The values of φ_i, φ_{i+1} = -5°, -5°, when perpetuated, would result in "chain closure" after about 24 units. Figure 2 shows that the minima in the energy surface for the meso, tt state occur at $(\varphi_i, \varphi_{i+1})$ = (10°, -15°) and (-15°, 10°). Perpetuation of such conformations would lead to right- and left-handed helices with 14 monomers per turn, with a repeat distance of 30.4 Å. It is known[17,18] that in the crystalline state, i-PMMA occurs in a helical form with n = 10 and pitch = 21.12 Å. This conformation has been shown[19] to be of lower energy than the five-fold helix proposed previously. It is likely that such helical segments occur in solution. Precedence to this proposal can be found in the interpretation of the solution properties of chains such as isotactic polystyrene and polypropylene in terms of segments of the threefold helical conformation.

Calculated values of C_∞, with φ_i, φ_{i+1} = 10°, -15° for the meso, tt state are also shown in Figure 5 (dashed curves). Comparing the curves, e.g., for E_β = -0.5 kcal mol^{-1}, calculations with 10°, -15° result in higher values of C_∞. Agreement with experimental values is achieved with $E_\alpha \approx 1000$, $E_\beta \approx -1000$, and E_ρ = 1000 cal mol^{-1}. Thus, while the loop-forming tendency of the conformation with (-5°, -5°) reduces C_∞, the extended helical segments promoted by conformations with (10°, -15°) increase its value.

A similar situation exists in the meso, gg state. Minima occur at (135°, 105°) and (105°, 135°), while $\langle \varphi_i, \varphi_{i+1} \rangle$ = (119.3, 119.3). The latter has been used in the calculations above. The conformation with (120°, 120°) would cause "chain closure" in three units. However, the perpetuation of $(\varphi_i, \varphi_{i+1})$ = (135°, 105°) and (105°, 135°), would lead to right- and left-handed helices, respectively, with n = 3.23 and pitch = 2.23 Å. Calculations were not performed with $(\varphi_i, \varphi_{i+1})$ = (105°, 135°) since the change in C_∞ is expected to be small due to the low incidence of the gg state.

Calculations may perhaps be extended, with statistical weight matrices comprising more than three states (t, g, $\bar{g}$) so as to include the "split" minima in states such as tt and gg. However, this is not attempted here. Since $(\varphi_i, \varphi_{i+1})$ = (10°, -15°) and (-15°, 10°) would lead to right- and left-handed helices with the same pitch and the same number of monomers per turn, the final value of C_∞ would not be affected by treating the meso, tt conformation as a single state with $(\varphi_i, \varphi_{i+1})$ = (10, -15°).

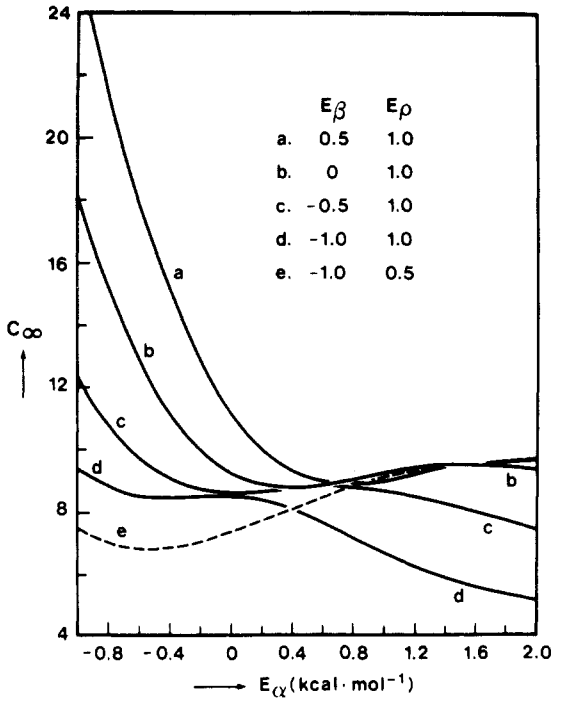

Figure 6. The characteristic ratio for syndiotactic PMMA is shown as a function of E_α for select values of E_β and E_ρ.

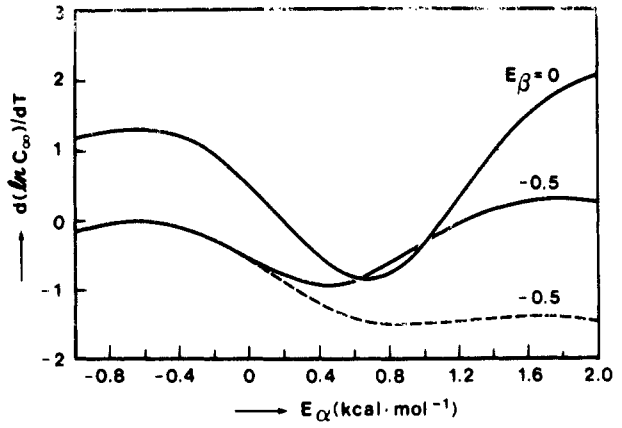

Figure 7. The temperature coefficient of the characteristic ratio for isotactic PMMA, at 300 K, is shown as a function of E_α for select values of E_β marked on the curves, with E_ρ = 1000 cal mol^{-1}. The solid curves were calculated with φ_i, φ_{i+1} = (-5°, -5°) for the meso, tt state, and the dashed curve, with φ_i, φ_{i+1} = 10°, -15°.

Plots of C_∞ as a function of E_α, for select values of E_β, are shown in Figure 6 for the syndiotactic chain. The value of C_∞ varies drastically with E_α up to E_α = 0, when E_β = 0.5 or 0 kcal mol^{-1}. The racemic, tt state depends on β. With $\langle\varphi_i, \varphi_{i+1}\rangle$ = (1.7°, 1.7°) in the tt state, the chain will have the tendency to form loops as discussed above. When $E_\beta \geq 0$ and $E_\alpha \leq 0$, the enhanced population of the gauche states suppresses the tendency for loop formation, leading to large C_∞. However, with $E_\beta < 0$, the increased population of the tt state reduces the value of C_∞. Experimental values of the characteristic ratio for predominantly syndiotactic chains are in the range of 6.5–8.4. This range is reproduced by $E_\alpha \approx 0.8$, E_β = -0.5 to -1.0, and E_ρ = 1 kcal mol^{-1}. Although, from Figure 6, it is seen that values of E_α in the range of -1.0 to 0 kcal mol^{-1} result in C_∞ = 7–8, the negative values of E_α do not reproduce the experimental C_∞ measured for isotactic PMMA chains.

The temperature coefficients, d(ln C_∞)/dT, calculated for the isotactic and syndiotactic PMMA are shown in Figures 7 and 8, respectively, for various values of the

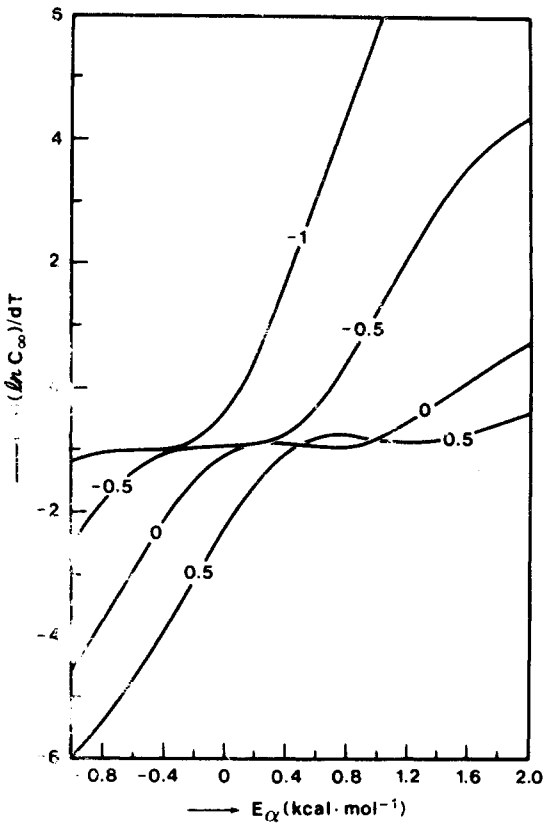

Figure 8. The temperature coefficient of the characteristic ratio for syndiotactic PMMA, at 300 K, is plotted as a function of E_α for select values of E_β and with E_ρ = 1.0 kcal mol^{-1}.

statistical weight parameters. In Figure 7, the sign of the temperature coefficient of C_∞ for the i-PMMA chain, calculated with $\langle\varphi_i, \varphi_{i+1}\rangle$ = (-5°, -5°) for the tt state, depends on the values of E_α and E_β. With E_α = 0.6–0.8 and E_β = 0 to -0.5 kcal mol^{-1}, d(ln C_∞)/dT is -0.9×10^{-3} K^{-1}. With $(\varphi_i, \varphi_{i+1})$ = (10°, -15°) for the tt state, the temperature coefficient is -1.5×10^{-3} K^{-1} with E_α = 0.8, E_β = -0.5 and E_ρ = 1 kcal mol^{-1}. The experimental value[20] of the temperature coefficient for i-PMMA is -2.3×10^{-3} K^{-1}. In view of the uncertainty in the experimental determination of this parameter, the approximations involved in the theoretical calculations, and the fact that the calculations were performed for a 100% isotactic chain, the agreement between the calculated and experimental values can be considered reasonable. It should be noted that the use of $(\varphi_i, \varphi_{i+1})$ = (10°, -15°), the perpetuation of which leads to helical segments, results in large negative values for the temperature coefficient.

The dependence of d(ln C_∞)/dT with E_α is shown for s-PMMA in Figure 8. It is seen that the temperature coefficient depends significantly on E_α and E_β. The experimental results from the work of five groups[20-24] on the temperature coefficient varies from 0 to 4.0×10^{-3} K^{-1}. It is seen from Figure 8 that such diverse values of this parameter are accounted for by E_α = 0.6–1.0 and E_β = -0.5 to -1.0 kcal mol^{-1}.

Stereoirregular Chains

Characteristic ratios, as a function of isotacticity w_m of the chain, were calculated with Monte Carlo chains of 200 units, and the average was taken over 25 such chains. The standard deviations in the characteristic ratios were less than 0.5. The results are shown in Figure 9 for select values of the statistical weight parameters. Two sets of curves are shown, with $\langle\varphi_i, \varphi_{i+1}\rangle$ = (-5°, -5°) and $(\varphi_i, \varphi_{i+1})$ = (10°, -15°), respectively for the meso, tt state. Generally,

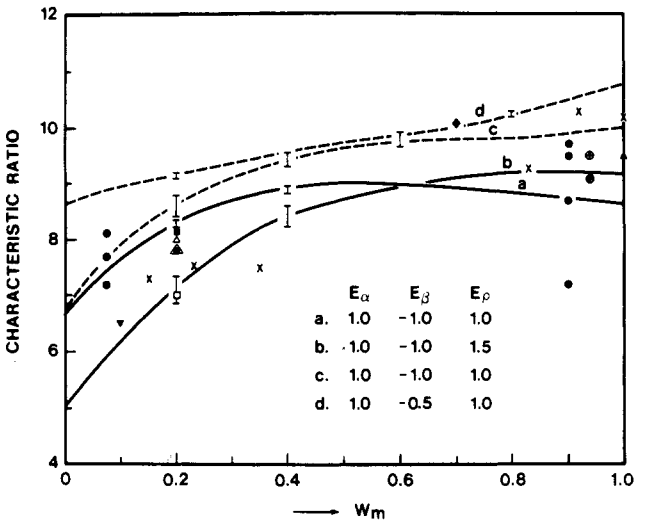

Figure 9. The characteristic ratios for PMMA, as a function of isotacticity, w_m, are shown for select values of the statistical weight parameters. The solid curves were calculated with $\varphi_i, \varphi_{i+1} = (-5°, -5°)$ for meso, tt state and the dashed curves, with $\varphi_i, \varphi_{i+1} = 10°, -15°$. The experimental values taken from Jenkins and Porter[7,8] are marked: (●) Sakurada et al; (▲) Katime et al.; (▼) Katime and Roig; (■) Fox; (△) Chinai; (□) Vasudevan and Santappa; (◆) Krause; (⊕) Schulz; (×) Jenkins and Porter.

a significant increase in C_∞ is noted as w_m increases from 0 to 0.4. Values of C_∞ in the range 9.5–11 are obtained for isotactic chains, when $(\varphi_i, \varphi_{i+1}) = (10, -15°)$ is used for the meso, tt state. The experimental results of various authors are shown in this figure. These were taken from the review of Jenkins and Porter[7] and their recent work.[8] It is seen that most experimental values of C_∞ for predominantly syndiotactic chains are reproduced by curves a and b, with $E_\alpha = 1$, $E_\beta = -1.0$, $E_\rho = 1$–1.5 kcal mol^{-1}, and $\langle \varphi_i, \varphi_{i+1} \rangle = (-5°, -5°)$ for the meso tt state. Some of the experimental values for isotactic chains are also consistent with curves a and b. The higher values of C_∞ for the isotactic chains are reproduced by curves c and d with $(\varphi_i, \varphi_{i+1}) = (10°, -15°)$. It is reasonable to expect that the perpetuation of helical segments promoted by $(\varphi_i, \varphi_{i+1}) = (10°, -15°)$ occurs when w_m is fairly large.

Acknowledgment. The author is grateful to Drs. M. Vacatello and P. J. Flory for kindly making available a copy of their manuscript "Conformational Statistics of Poly(methyl methacrylate)", submitted concurrently with this paper. It differs from the present treatment in allowing for variations in the bond angle θ' and in accommodating the split minima in a six-state statistical weight matrix scheme.

Registry No. PMMA (homopolymer), 9011-14-7; isotactic-PMMA (homopolymer), 25188-98-1; syndiotactic-PMMA (homopolymer), 25188-97-0.

References and Notes

(1) Sundararajan, P. R.; Flory, P. J. *J. Am. Chem. Soc.* **1974**, *96*, 5025.
(2) Sundararajan, P. R. *J. Polym. Sci., Polym. Lett. Ed.* **1977**, *15*, 699.
(3) Yoon, D. Y.; Flory, P. J. *Polymer* **1975**, *16*, 645.
(4) Lovell, R.; Windle, A. H. *Polymer* **1981**, *22*, 175.
(5) Birshtein, T. M.; Merkur'yeva, A. A.; Goryunov, A. N. *Polym. Sci. USSR (Engl. Transl.)* **1983**, *25*, 143.
(6) Yoon, D. Y.; Flory, P. J. *J. Polym. Sci., Polym. Phys. Ed.* **1976**, *14*, 1425.
(7) Jenkins, R.; Porter, R. S. *Adv. Polym. Sci.* **1980**, *36*, 1.
(8) Jenkins, R.; Porter, R. S. *Polymer* **1982**, *23*, 105.
(9) O'Reilly, J. M.; Mosher, R. A. *Macromolecules* **1981**, *14*, 602.
(10) O'Reilly, J. M.; Teegarden, D. M.; Mosher, R. A. *Macromolecules* **1981**, *14*, 1693.
(11) Suter, U. W.; Flory, P. J. *Macromolecules* **1975**, *8*, 765.
(12) Sundararajan, P. R. *Macromolecules* **1977**, *10*, 623.
(13) Yoon, D. Y.; Sundararajan, P. R.; Flory, P. J. *Macromolecules* **1975**, *8*, 776.
(14) Sundararajan, P. R. *Macromolecules* **1980**, *13*, 512.
(15) Flory, P. J.; Sundararajan, P. R.; DeBolt, L. C. *J. Am. Chem. Soc.* **1974**, *96*, 5015.
(16) Flory, P. J. *Macromolecules* **1974**, *7*, 381.
(17) Kusanagi, H.; Tadokoro, H.; Chatani, Y. *Macromolecules* **1976**, *9*, 531.
(18) Bosscher, F.; Brinke, G. T.; Eshuis, A.; Challa, G. *Macromolecules* **1982**, *15*, 1364.
(19) Sundararajan, P. R. *Macromolecules* **1979**, *12*, 575.
(20) Sakurada, I.; Nakajima, A.; Yoshizaki, O.; Nakamae, K. *Kolloid Z.* **1962**, *186*, 41.
(21) Fox, T. G. *Polymer* **1962**, *3*, 111.
(22) Vasudevan, P.; Santappa, M. *J. Polym. Sci., Part A-2* **1971**, *9*, 483.
(23) Schulz, G. V.; Kirste, R. *Z. Phys. Chem.* **1961**, *30*, 171. Schulz, G. V.; Wunderlich, W.; Kirste, R. *Makromol. Chem.* **1964**, *75*, 22.
(24) Moore, W. R.; Fort, R. F. *J. Polym. Sci., Part A* **1963**, *1*, 929.